

# Hydroxyl Radical Mediated Degradation of Phenylarsonic Acid

Tielian Xu,<sup>†</sup> Prashant V. Kamat,<sup>‡</sup> Sachin Joshi,<sup>†</sup> Alexander M. Mebel,<sup>†</sup> Yong Cai,<sup>†</sup> and Kevin E. O'Shea<sup>\*,†</sup>

Department of Chemistry and Biochemistry, Florida International University, Miami, Florida 33199, and Radiation Laboratory and Department of Chemistry and Biochemistry, University of Notre Dame, Notre Dame, Indiana 46556

Received: March 16, 2007; In Final Form: June 7, 2007

Phenyl-substituted arsonic acids have been widely used as feed additives in the poultry industry. While very few studies have been reported on the environmental impact of these compounds, they have been introduced into the environment through land application of poultry litter in large quantities (about 10<sup>6</sup> kg/year). Phenylarsonic acid (PA) was used as a model for problematic arsonic acids. Dilute aqueous solutions of PA were subjected to  $\gamma$  radiolysis under hydroxyl radical generating conditions, which showed rapid degradation of PA. Product studies indicate addition of  $\cdot\text{OH}$  to the phenyl ring forms the corresponding phenols as the primary products. Arsenite,  $\text{H}_3\text{As}^{\text{III}}\text{O}_3$ , and arsenate,  $\text{H}_3\text{As}^{\text{V}}\text{O}_4$ , were also identified as products. The optimized structures and relative calculated energies (using GAUSSIAN 98, the B3LYP/6-31G(d) method) of the various transient intermediates are consistent with the product studies. Pulse radiolysis was used to determine the rate constants of PA with  $\cdot\text{OH}$  ( $k = 3.2 \times 10^9 \text{ M}^{-1} \text{ s}^{-1}$ ) and  $\text{SO}_4^{\cdot-}$  ( $k = 1.0 \times 10^9 \text{ M}^{-1} \text{ s}^{-1}$ ). PA reacts slower toward  $\text{O}^{\cdot-}$  ( $k = 1.9 \times 10^7 \text{ M}^{-1} \text{ s}^{-1}$ ) and  $\text{N}_3^{\cdot}$  (no detectable transient), due to the lower oxidation potential of these two radicals. Our results indicate advanced oxidative processes employing  $\cdot\text{OH}$  and  $\text{SO}_4^{\cdot-}$  can be effective for the remediation of phenyl-substituted arsonic acids.

## 1. Introduction

Arsenic is present in natural waters in both inorganic and organic forms. Although the inorganic species are predominant, the presence of organoarsenic compounds, such as methyl and phenyl arsenic compounds, have been reported.<sup>1,2</sup> Of particular interest is phenyl-substituted arsonic acids, which are used in agriculture to control cecal coccidiosis in poultry, to promote growth, to provide improved feed conversion, to better feather, and to increase egg production and pigmentation.<sup>3</sup> 4-Hydroxy-3-nitrophenylarsonic acid (roxarsone), *p*-arsanilic acid, 4-nitrophenylarsonic acid, *p*-ureidophenylarsonic acid, and phenylarsonic acid, shown in Scheme 1, are commonly utilized in the broiler poultry industry as feed additives. Large quantities of arsenic are introduced into the environment through land application of poultry litter containing these arsonic acids, especially roxarsone. Approximately 70% of broiler chickens produced in the U.S. are fed roxarsone, which is excreted largely unaltered into the environment.<sup>4,5</sup> Approximately 10<sup>6</sup> kilograms/year (kg/year) of roxarsone and its degradation products are introduced annually into the environment from the application of poultry litter onto agricultural fields near chicken houses.<sup>3</sup> A better understanding of the environmental impact and the ultimate fate of organoarsenicals applied to soils and other ecosystems is of significant importance.<sup>1,6</sup>

Advanced oxidation processes (AOPs), such as ultrasonic irradiation, photocatalysis, UV/H<sub>2</sub>O<sub>2</sub>, are radical-mediated processes that are effective for the treatment of inorganic arsenic species, in water.<sup>7–16</sup> In this paper the inorganic arsenic species, arsenite,  $\text{H}_3\text{As}^{\text{III}}\text{O}_3$ , and arsenate,  $\text{H}_3\text{As}^{\text{V}}\text{O}_4$ , will be referred to as As(III) and As(V), respectively. Only a limited number of

reports have appeared on the treatment of arsonic acids by AOPs. For example, attempts have been made to use hydrothermal and photocatalytic processes for the remediation of phenylarsonic acid disposed in Japan during World Wars I and II.<sup>17,18</sup>

Hydroxyl radical is generally considered to be the reactive species responsible for degradation of target compounds (pollutants) during AOPs. It is a powerful oxidant, especially important in environmental and biological systems.<sup>19,20</sup> Hydroxyl radical has been extensively studied for environmental remediation of organic and inorganic pollutants.<sup>21,22</sup> While the oxidation of inorganic arsenic with hydroxyl radicals has been carefully investigated,<sup>23</sup> the mechanistic details for reaction of hydroxyl radicals with arsonic acid species have not been reported. A detailed understanding of the reactivity of arsonic acids toward oxidative radicals is required to assess the potential applications of AOPs for their remediation. Such studies are relevant to the environmental fate and metabolism of arsonic acid, which often involve the same type of oxidative processes as observed in AOPs.

Pulse and  $\gamma$  radiolysis studies were conducted to obtain the mechanistic and kinetic details of hydroxyl radical mediated oxidation of phenylarsonic acid (PA), a model for the phenylarsonic acid substrates of environmental concern.

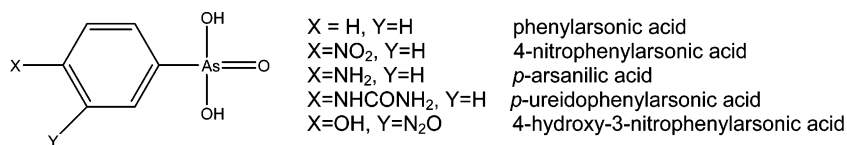
## 2. Experimental Section

**2.1. Materials.** PA was purchased from Avocado (97% purity) and used as received. 2-Hydroxyphenylarsonic acid was purchased from Sigma, and 4-hydroxyphenylarsonic acid is from TCI, America. All other chemicals were purchased from Aldrich or Fisher and used without further purification. All the experiments were performed at room temperature using 18 M $\Omega$  deionized water.

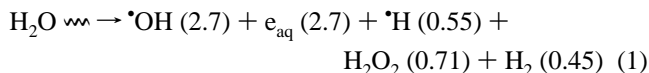
\* Corresponding author.

<sup>†</sup> Florida International University.

<sup>‡</sup> University of Notre Dame.

**SCHEME 1: Structures of Phenyl-Substituted Arsonic Acids**

**2.2. Radiation Chemistry.** Irradiation of dilute aqueous solutions (<0.1 M) with high-energy radiation leads to the production of reactive free radicals, OH radicals, hydrated electrons and H atoms, and molecular products H<sub>2</sub>O<sub>2</sub> and H<sub>2</sub>,



where the values in parentheses indicate the yield as *G* values that represent the number of species per 100 eV deposited energy. The *G* values listed in reaction 1 refer to measured yields in dilute substrate solutions and can be converted into SI units by multiplying with the factor  $1.036 \times 10^{-7} \text{ mol J}^{-1}$ .

The OH radical is a very strong oxidant ( $E_0 = 1.9 \text{ V}$  vs NHE). In nitrous oxide (N<sub>2</sub>O) saturated solutions, the solvated electrons  $e_{\text{aq}}^-$  are selectively converted to  $\cdot\text{OH}$  radicals with a bimolecular rate constant of  $9.1 \times 10^9 \text{ M}^{-1} \text{ s}^{-1}$  according to

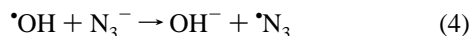


A system consisting of 90% OH radicals and 10% H atoms is achieved under these conditions with  $G(\cdot\text{OH}) = 5.4$  and  $G(\cdot\text{H}) = 0.55$ , thus nearly doubling the amount of  $\cdot\text{OH}$  for reaction.<sup>24</sup> The concentration of  $\cdot\text{OH}$  was 4.0–4.5  $\mu\text{M}$  during this study.

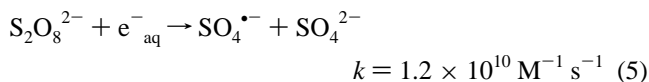
The study of the  $\text{O}^{\cdot-}$  reactions was carried out in N<sub>2</sub>O saturated solutions at pH 13.4 adjusted with 0.1 M NaOH. Under these basic conditions, approximately 97% OH radicals are converted to  $\text{O}^{\cdot-}$ , according to



Azide radical,  $\cdot\text{N}_3$ , is a mild oxidant with oxidation potential of 1.33 V vs NHE at pH 7.<sup>25</sup> It is more selective than hydroxyl radical, primarily reacting as a one-electron oxidant (not via H-abstraction) with the primary formation of radical cations.<sup>26</sup>  $\cdot\text{N}_3$  was formed by employing relatively high concentrations of sodium azide (0.01 M) to scavenge  $\cdot\text{OH}$  radicals under N<sub>2</sub>O saturation with a rate constant of  $1.2 \times 10^9 \text{ M}^{-1} \text{ s}^{-1}$ .



The sulfate radical  $\text{SO}_4^{\cdot-}$  is a very strong oxidant ( $E_0 = 2.5$ – $3.1 \text{ V}$  vs NHE) and typically reacts with organic substrates by one electron transfer.<sup>27</sup> Radiolytic generation of  $\text{SO}_4^{\cdot-}$  was accomplished by the reaction of persulfate dianion (5 mM) with solvated electron in N<sub>2</sub>-saturated solutions.



Under these conditions, the hydroxyl radical was scavenged by 0.05 M *tert*-butyl alcohol (eq 6;  $k = 7.6 \times 10^8 \text{ M}^{-1} \text{ s}^{-1}$ ),<sup>28</sup> and the yield of  $\text{SO}_4^{\cdot-}$  was  $G(\text{SO}_4^{\cdot-}) = 2.7$ .



The rate constants determined in this paper were obtained by plotting the average of the data points employing Origin

software (Version 7). Least-squares linear regression was applied to the data, with  $R^2$  as a measure for the quality of the fit.

**Pulse Radiolysis.** Pulse radiolysis experiments were carried out using the Notre Dame 8 MeV Titan Beta model TBS-8/16-1S linear accelerator with a pulse length of 2.5–10 ns at the Radiation Laboratory, University of Notre Dame. Detailed descriptions of the instrument setup, as well as the basic details of the experiment and data analysis, have been given elsewhere.<sup>29,30</sup> A typical experiment consisted of a series of 6–10 replicate shots, which were averaged for a single measurement. Dosimetry was carried out with N<sub>2</sub>O-saturated solutions of 10 mM KSCN assuming  $\epsilon_{472 \text{ nm}} = 7580 \text{ M}^{-1} \text{ cm}^{-1}$  and  $G = 6.13$  for (SCN)<sup>2-</sup>.<sup>31</sup>

**$\gamma$  Radiolysis.** The  $\gamma$  radiolysis experiments were performed in a Shepherd Cobalt 60 source. The dose rate was 117 Gy/min, as determined by Fricke dosimetry. Glass vials (Fisher-brand, 19  $\times$  65 mm<sup>2</sup>) were filled with 10 mL of 1.0 mM PA solution, sealed with rubber septa, and purged with N<sub>2</sub>O gas for 5 min prior to irradiation. To study the degradation as a function of irradiation time, a sufficient number of samples was placed in the <sup>60</sup>Co source. Samples were removed at different irradiation times for product analyses.

**2.3. Analysis.** Arsenic species were analyzed by continuous high-performance liquid chromatography (HPLC) in conjunction with inductively coupled plasma-mass spectrometry (ICP-MS) detection. The HPLC (Spectra System P4000 with a AS 3000 autosampler) was fitted with an anion-exchange column (Dionex IonPac AS7, 250 mm  $\times$  4 mm i.d., 5  $\mu\text{m}$  particle size) through which the mobile phase (50 mM HNO<sub>3</sub>) was passed at a flow rate of 1.0 mL min<sup>-1</sup>. The sample injection volume was 100  $\mu\text{L}$ . The ICP-MS (HP4500 Plus) was controlled using HP ChemStation Software WinNT. The plasma and auxiliary gas flow rate for the ICP-MS were maintained at 15.9 and 1.04 L/min, respectively.

The analyses for phenol were conducted using Beckman HPLC equipped with a diode array detector and an ODS2 C-18 reverse phase column (250 mm  $\times$  4.6 mm). The eluant was a mixture of methanol and water (60:40) at a flow rate of 1 mL/min.

The LC-MS system used in the study consisted of a Finnigan Spectra System P4000 HPLC pump and Finnigan Spectra System AS 3000 autosampler and a Thermoquest Navigator mass spectrometer with electrospray ionization source. The mass spectra data were obtained in the negative ion mode by full scanning from *m/z* 60 to 1000.

**2.4. Computational Methods.** Geometries of adducts from the reaction of hydroxyl radical with phenylarsonic acid (deprotonated monoanionic form) have been optimized at the hybrid density functional B3LYP level<sup>32,33</sup> with the 6-31G(d) basis set. Vibrational frequencies of all species were computed using the same B3LYP/6-31G(d) method for characterization of the optimized structures as local minima or transition states and to obtain zero-point vibrational (ZPVE) corrections. Single-point energies were then refined at the B3LYP level with the larger G3Large basis set developed by Curtiss et al. for Gaussian-3 calculations of molecules containing first-, second-,

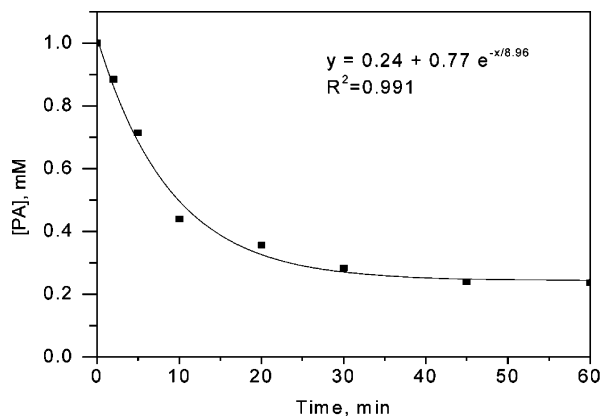


**Figure 1.** Degradation of PA (1.0 mM) in  $N_2O$ -saturated solution at a dose rate of 117 Gy/min under  $\gamma$  radiolysis.

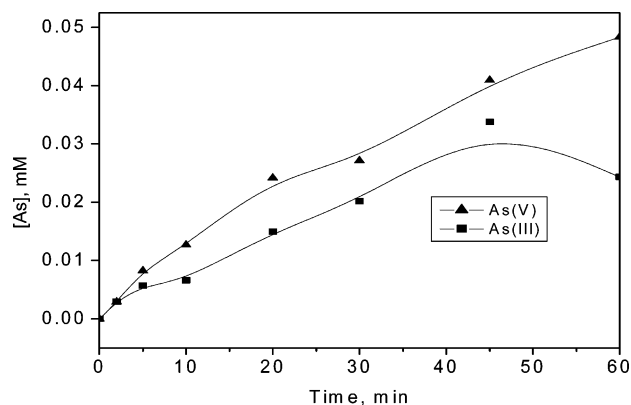


**Figure 2.** Evolution of the inorganic arsenic As(III) and As(V) during the radiolysis of PA ( $[PA]_0 = 1.0$  mM) under  $N_2O$ -saturated condition observed from HPLC-ICP-MS.

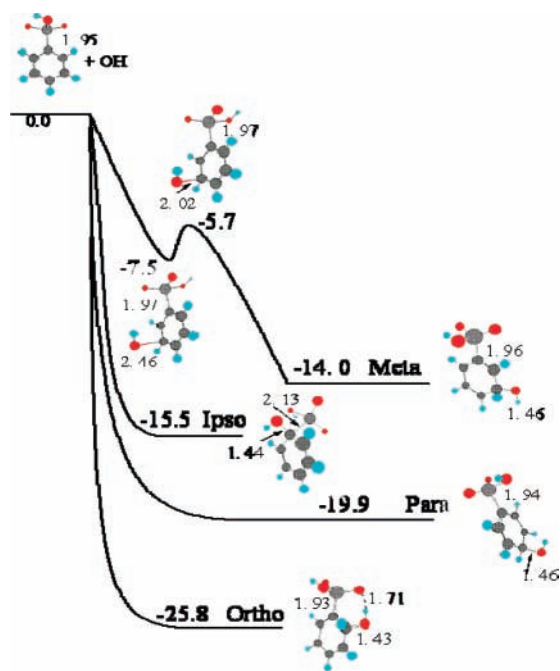


**Figure 3.** Potential energy profile of the  $C_6H_5As(OH)(O)(O)^- + \bullet OH \rightarrow C_6H_5(OH)As(OH)(O)(O)^-$  reaction calculated at the B3LYP/G3Large//6-31G(d) + ZPE(B3LYP/6-31G(d)) level of theory. The numbers specify relative energies in kilocalories per mole. Selected C–(OH) and C–As distances are shown in angstroms.

and third-row  $sp$  elements.<sup>34</sup> All calculations were performed using the GAUSSIAN 98 quantum chemistry program package.<sup>35</sup>

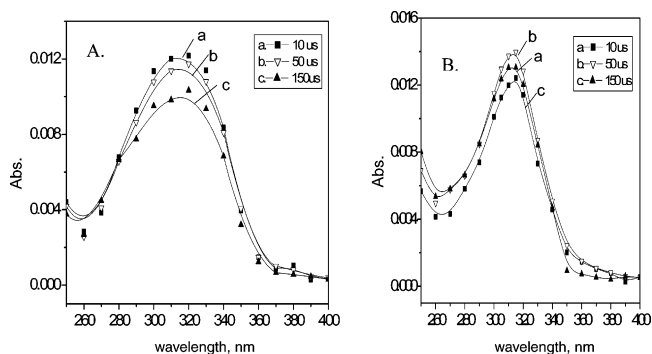


**Figure 4.** Time-resolved absorption spectrum of the transients formed after the pulse radiolysis of an  $N_2O$ -saturated solution of PA (1.0 mM) at (A)  $pH = 7.0 \pm 0.2$  and (B)  $pH = 13.4 \pm 0.2$ .

### 3. Results and Discussion

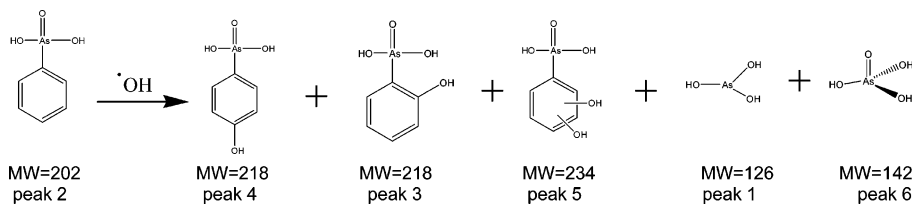
**3.1.  $\gamma$  Radiolysis.** The first step in our study was to identify the products formed in the oxidation reaction of PA with hydroxyl radical. PA is highly susceptible to attack by  $\bullet OH$ . Figure 1 shows the degradation of PA during  $\gamma$  radiolysis. The decay fits to a single-exponential decay with a half-life of  $\sim 9.0$  min for the degradation of PA under our experimental conditions. The decrease in the degradation at longer irradiation times is likely the result of reaction products competing with PA for hydroxyl radical.

Products from the reaction of PA with  $\bullet OH$  were identified using HPLC-ICP-MS. The HPLC analysis of the reaction mixture following the  $\gamma$  radiolysis of the PA solution after 20 min irradiation yields six major peaks. On the basis of matching retention times and correlation by spiking the authentic compounds, the peaks were assigned as follows; peak 1 = As(III) (150 s), peak 2 = PA (310 s), peak 3 = 2-hydroxylphenylarsonic acid (370 s), peak 4 = 4-hydroxylarsonic acid (400 s), peak 5 = unknown (500 s), and peak 6 = As(V) (590 s). Although 3-hydroxyl- or dihydroxyl-substituted isomers are not commercially available for confirmation, peak 5 may correspond to one of these expected products (Scheme 2).

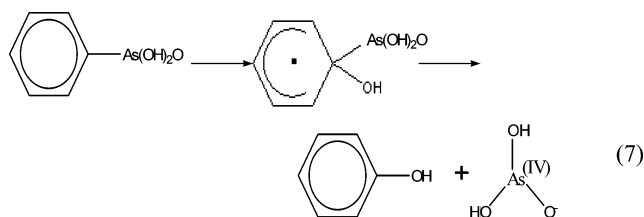
To further identify and confirm these products, electrospray MS analysis (direct infusion) was conducted for the PA solution following 20 min irradiation. Peaks corresponding to PA (MW = 202) at  $m/z = 201$ , As(III) ( $m/z = 125$ ), As(V) ( $m/z = 141$ ), and monohydroxylated phenylarsonic acids ( $m/z = 217$ ) are observed. An observed peak with  $m/z = 233$  is assigned to a dihydroxylated phenylarsonic acid (MW = 234) and corresponds to peak 5 from the HPLC-ICP-MS analysis. At the initial stages of the reaction, the primary products appear to be monohydroxylated phenylarsonic acid ( $m/z = 217$ ). The concentration of the monohydroxylated adducts does not increase substantially with irradiation time, because these products are more electron-rich, more reactive, and thus oxidized more quickly than the starting material. Although an authentic sample of 3-hydroxyphenylarsonic acid was not available, the chromatographic behavior and MS analyses of authentic 2- and 4-hydroxyphenylarsonic acids match with reaction products assigned to peaks 3 and 4 from the HPLC-ICP-MS analysis.

In addition to the hydroxylated ring products, As(III) and As(V) were also formed during hydroxyl radical oxidation of PA. While the inorganic arsenic species are often more toxic than organic arsenic species,<sup>36</sup> there are a number of remediation methods available for removal of inorganic arsenic.<sup>37–40</sup> The observed inorganic arsenic species indicates cleavage of the As–C bond during the reaction of PA with hydroxyl radical. The initial formation of As(III) and As(V) occurs at ap-

## SCHEME 2: Products from Reaction of PA with Hydroxyl Radical



proximately 1:1 ratio (Figure 2), which is consistent with the disproportionation of an As(IV) intermediate. As(IV) disproportionates to As(III) and As(V) at a nearly diffusion controlled rate.<sup>23</sup> To explain the formation of As(IV), we propose ipso-addition of hydroxyl radical followed by homolytic cleavage of the As–C bond, yielding unstable As(IV) species, eq 7. The presence of phenol in the reaction solution was also confirmed by HPLC analysis. As(IV) will rapidly disproportionate into the observed 1:1 ratio of As(III) and As(V).



At longer irradiation times, the concentration of As(V) increases with a simultaneous decrease of As(III). Under our radiolytic conditions relatively high concentrations of  $\bullet\text{OH}$  radicals are produced (4.0–4.5  $\mu\text{M}$ ) which can directly oxidize As(III) ( $k = 8.5 \times 10^9 \text{ M}^{-1} \text{ s}^{-1}$ ). As(V) can also be formed by extensive oxidation of the aromatic ring. Under continued irradiation, As(V), the less toxic form, accumulates as the final product of arsenic species of PA mineralization.

Computational methods were used to further explore the reaction pathways and the energies of probable transients during the reaction of PA with  $\bullet\text{OH}$ . The  $\text{p}K_{\text{a}}$ 's of PA are 3.8 and 8.5. Studies were conducted under neutral conditions where PA exists as monoanion  $\text{C}_6\text{H}_5\text{As}(\text{OH})(\text{O})(\text{O})^-$ . The calculated potential energy diagram for the  $\text{C}_6\text{H}_5\text{As}(\text{OH})(\text{O})(\text{O})^- + \bullet\text{OH}$  reaction leading to *ipso*-, *o*-, *m*-, and *p*- $\text{C}_6\text{H}_5(\text{OH})\text{As}(\text{OH})(\text{O})(\text{O})\bullet^-$  adducts is depicted in Figure 4. The addition of the  $\bullet\text{OH}$  radical to deprotonated phenylarsonic acid is exothermic and takes place without a barrier. The ortho- and para-adducts are found to be the most stable, 25.8 and 19.8 kcal/mol below the reactants, respectively, consistent with product studies. The transient leading to ortho-structure appears to be further stabilized by intermolecular hydrogen bonding between the OH group in the ortho-position in the benzene ring and an oxygen atom; the hydrogen bond  $\text{As}-(\text{OH})\cdots(\text{H})$  distance is calculated to be 1.71 Å. The ipso-adduct is exothermic by 15.5 kcal/mol. For the ipso-adduct the OH and As groups are attached to the same carbon and the C–As bond is expected to be the weakest among the adducts, as indicated by the longest C–As distance, 2.13 Å, compared to a bond length of 1.93–1.96 Å for the other adducts. This result supports our proposed mechanism leading to the inorganic arsenic species (eq 7). All four OH addition reactions are calculated to be barrier-less with respect to the reactants,  $\text{C}_6\text{H}_5\text{As}(\text{OH})(\text{O})(\text{O})^- + \bullet\text{OH}$ . Therefore, their rate constants are controlled by the attractiveness of the potential energy profile when the OH radical approaches different sites in phenylarsonic acid. As shown in Figure 3, the potential is most attractive for the ortho-addition, followed by para-, ipso-, and meta-additions, thus determining the kinetic preference of

the different addition sites. The computational results indicate that the formation of the meta-isomer occurs in two steps: the formation of a weakly bound (by 7.5 kcal/mol) complex followed by rearrangement to the meta-adduct (Figure 4). The second step exhibits a barrier of 1.8 kcal/mol, but the corresponding transition state resides 5.7 kcal/mol lower than the reactants. The presence of such a “bump on the road” is likely to slow down the production of the meta-isomer as compared to the other adducts. We could not gather experimental evidence for the formation of the meta-isomer from the  $\gamma$  radiolysis product studies.

**3.2. Pulse Radiolysis. Reaction with  $\bullet\text{OH}$  Radicals.** Pulse radiolysis was used to determine the kinetic parameters and monitor transient species. The experiments were carried out in  $\text{N}_2\text{O}$ -saturated aqueous solution.  $\text{N}_2\text{O}$  converts electrons to  $\bullet\text{OH}$  radicals resulting in >90% selective production of  $\bullet\text{OH}$ . The hydroxyl radical is highly reactive toward aromatic and heterocyclic compounds, and it usually adds to the aromatic ring to form the hydroxycyclohexadienyl radical with a characteristic absorption in the 310–350 nm range.<sup>41,42</sup> The time-resolved transient absorption spectra of PA (1.0 mM, pH = 7.0  $\pm$  0.2) recorded 10, 50, and 150  $\mu\text{s}$  after pulse radiolysis under hydroxyl radical generating conditions are shown in Figure 4A. The spectra show a broad peak around 320 nm. The growth in the adsorption at this wavelength represents the formation of a transient species from the reaction of PA with  $\bullet\text{OH}$  radical. The growth of the transient species was analyzed with pseudo-first-order kinetics at different concentrations of PA (0.12–1.0 mM). The bimolecular rate constant for the reaction of PA with  $\bullet\text{OH}$ , determined from the linear dependence of the pseudo-first-order growth rate constant on the PA concentration, is  $(3.2 \pm 0.1) \times 10^9 \text{ M}^{-1} \text{ s}^{-1}$  at 320 nm. This value indicates that the  $\bullet\text{OH}$  radical attack on PA occurs at a nearly diffusion controlled rate. The decay of the transient follows first-order kinetics, with a half-life of 0.54 ms. Similar growth and decay rates at different wavelengths between 300 and 320 nm indicate the involvement of single transient intermediate at pH 7.

In the aqueous solutions, the reaction of  $\bullet\text{OH}$  radicals can undergo a variety of reactions (abstraction, addition, and electron transfer).<sup>28,42,43</sup> The hydroxyl radicals typically react with benzene and substituted derivatives by an addition reaction forming hydroxycyclohexadienyl type radicals. In electron-rich aromatic ring systems, the hydroxyl radicals and specific one-electron oxidants can undergo electron transfer and form a solute radical cation, especially when the substrate possesses electron-donating substituents such as  $-\text{CH}_3$  and  $-\text{OCH}_3$  groups.<sup>28</sup> Computational results indicate electron transfer between PA and the hydroxyl radical to form the radical cation is unlikely, being endothermic by 52 kcal/mol.

**Reaction with  $\text{O}^{\bullet-}$ .** Although the reactions of  $\text{O}^{\bullet-}$  have not been extensively studied, there has been an increased interest in its chemistry. Its contribution can be significant in the radiolytic chemistry of highly alkaline solutions. The time-resolved transient absorption spectra of PA (1.0 mM, pH = 13.4)

recorded following pulse radiolysis of a N<sub>2</sub>O-saturated aqueous solution are shown in Figure 4B.

While O<sup>•-</sup> and •OH exhibit similar hydrogen abstracting ability, O<sup>•-</sup> radical undergoes an electron-transfer oxidation with unsubstituted aromatics and abstracts a hydrogen from a number of methyl-substituted aromatics.<sup>44–46</sup> For PA, hydrogen abstraction is not an energetically feasible pathway. We expect O<sup>•-</sup>, a strong one-electron oxidant ( $E(O^{\bullet-}/O^{2-}) = 1.1$  V),<sup>47</sup> to react via addition as well as single-electron-transfer pathways.<sup>48</sup>

The bimolecular rate constant  $k_{\text{obs}}$  was determined by measuring the transient absorption growth constant (320 nm) at different PA concentrations. The slope of the linear plot of the growth rate constant versus PA concentration yields a  $k_{\text{obs}}$  of  $1.1 \times 10^8 \text{ M}^{-1} \text{ s}^{-1}$ . Both •OH and O<sup>•-</sup> collectively contribute to this value, and  $k_{\text{exp}}$  can be expressed in the form<sup>24</sup>

$$k_{\text{obs}} = \frac{k_{\text{OH}} + k_{\text{O}}(K_{\text{a}}/[H^+])}{1 + K_{\text{a}}/[H^+]} \quad (8)$$

where  $K_{\text{a}}$  is the acid-ionization constant of •OH, with the value  $1.3 \times 10^{-12}$  M.  $k_{\text{OH}}$  is the rate constant of •OH reaction with PA at 320 nm ( $k_{\text{OH}} = 3.2 \times 10^9 \text{ M}^{-1} \text{ s}^{-1}$ ). Substituting these experimental values into eq 8 yields a bimolecular rate constant for the reaction of PA with O<sup>•-</sup> of  $k_{\text{O}} = 1.9 \times 10^7 \text{ M}^{-1} \text{ s}^{-1}$ . This reduced reactivity relative to hydroxyl radical is due to the decreased electrophilicity of reacting radicals and the increased electrostatic repulsion between a negatively charged radical and the dianionic arsenate group in PA. Such relatively slow rate constants for the O<sup>•-</sup> reaction have been observed in the case of other aromatic and heterocyclic compounds.<sup>49,50</sup> The rate constant for the reaction O<sup>•-</sup> is more than 2 orders of magnitude (~170 times) slower than that for OH radical. Under these alkaline conditions there is only a 16% probability of the O<sup>•-</sup> reaction occurring, despite 32 times higher concentration of O<sup>•-</sup> than OH radical. The transient spectra recorded at pH 13.4 following radiolysis of a dilute aqueous solution of PA under N<sub>2</sub>O saturation results predominantly from the •OH addition adduct of PA.

**Reaction with Sulfate and Azide Radicals.** To obtain further insight into a possible electron-transfer mechanism, we investigated reactions of PA with other oxidizing radicals. The azide radical N<sub>3</sub><sup>•</sup> is a one-electron oxidant and typically participates in direct electron transfer (not addition) with aromatic compounds with the primary formation of radical cations.<sup>51</sup> The transient absorption spectra recorded following the reaction of N<sub>3</sub><sup>•</sup> radicals with PA does not possess any distinct adsorption peaks that can be assigned to a radical cation species.

Sulfate radical, a stronger one-electron oxidant ( $E_0 = 2.5$ – $3.1$  V vs NHE), typically reacts with aromatic compounds via direct electron transfer to form radical cations.<sup>43</sup> The time-resolved difference absorption spectra obtained following the reaction of SO<sub>4</sub><sup>•-</sup> with PA are shown in Figure 5. The transient absorption spectra obtained following the reactions of PA with •OH and SO<sub>4</sub><sup>•-</sup> are similar with a strong absorption band around 320 nm; however, in the case of SO<sub>4</sub><sup>•-</sup> a short-lived absorption band was observed at 390 nm immediately following the pulse which disappears within 1–5 μs. While this adsorption may be related to the radical cation product expected from the reaction of SO<sub>4</sub><sup>•-</sup> with PA, we were unable to further characterize the product because of its short lifetime. Aromatic radical cations in aqueous solution can be very short-lived and tend to undergo rapid hydrolysis to form the corresponding HO adducts.<sup>52–54</sup> The absorption spectra at short time scales did not allow for correlation of the kinetics for the disappearance of the initial

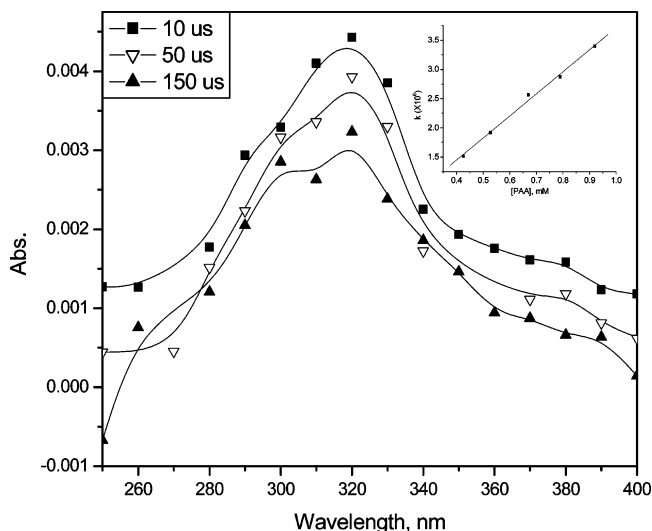
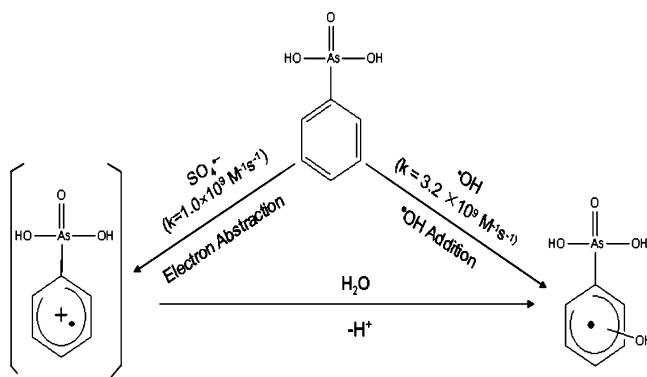


**Figure 5.** Time-resolved absorption spectra following oxidation of PA with SO<sub>4</sub><sup>•-</sup> at pH = 7.0 ± 0.2 (N<sub>2</sub>-purged 1.0 mM PA solutions containing 2% (v/v) *t*-BuOH, 10 mM K<sub>2</sub>S<sub>2</sub>O<sub>8</sub>, and 50 mM phosphate buffer). (Insert: Dependence of pseudo-first-order rate constant for the adsorption at 320 nm on the concentration of PA.)

### SCHEME 3: Proposed Mechanisms of Oxidative Radicals Reaction with PA



SO<sub>4</sub><sup>•-</sup> reaction products with the formation of the •OH product. On the basis of literature reports, we postulate that SO<sub>4</sub><sup>•-</sup> reacts with PA to form the radical cation which hydrolyzes to form the HO adduct.

The pseudo-first-order rate constant for the formation of the intermediate for the reaction of PA with sulfate radical was found to be  $1.0 \times 10^9 \text{ M}^{-1} \text{ s}^{-1}$  at the absorption maximum. This follows the trend that the rate constants for SO<sub>4</sub><sup>•-</sup> reaction are generally lower than those found for the •OH reaction and consistent with the relative reactivity of SO<sub>4</sub><sup>•-</sup> and •OH with aromatics.<sup>55</sup> The initial pathways for the reactions of SO<sub>4</sub><sup>•-</sup> and •OH with PA are proposed in Scheme 3.

## 4. Conclusions

Phenyl-substituted arsonic acids, introduced into the environment through agriculture activities in significant quantities, are problematic pollutants. The persistence of these compounds and their effects on animal and human health are of general concern. PA is used as a model for phenylated arsenic compounds to study their radical reactions. PA is very reactive toward the strong oxidants, hydroxyl radicals and sulfate radicals, occurring at near diffusion controlled rates. Computational and product studies suggest •OH preferentially adds at the ortho- and para-positions of PA, yielding 2- and 4-hydroxyl adducts as the initial products. Hydroxyl radical addition at the ipso-position is

proposed to lead to the formation of As(IV), which can disproportionate to As(III) and As(V). As(III) is oxidized to arsenate upon continued treatment with  $\bullet\text{OH}$ . The reactivity of  $\bullet\text{OH}$  observed under our experimental conditions may parallel such processes that occur during metabolism of these compounds and are relevant to their environmental fate. We have shown the  $\bullet\text{OH}$  readily degrades PA and treatment by AOPs ( $\bullet\text{OH}$  generating processes) can be used to mineralize arsonic acids.

**Acknowledgment.** K.E.O. gratefully acknowledges support from the NIH/NIEHS (Grant No. S11ES11181). T.X. is supported by a Dissertation Year Fellowship from the University Graduate School at FIU. We thank the reviewers for valuable insight and suggestions. P.V.K. acknowledges the support of the Office of Basic Energy Science of the Department of the Energy. This is Contribution No. NDRL 4738 from the Notre Dame Radiation Laboratory.

## References and Notes

- Jackson, B. P.; Bertsch, P. M. *Environ. Sci. Technol.* **2001**, *35*, 4868–4873.
- Pergantis, S.; Heithmar, E. M.; Hinners, T. A. *Analyst* **1997**, *122*, 1063–1068.
- Cortinas, I.; Field, J. A.; Kopplin, M.; Garbarino, J. R.; Gandolfi, A. J.; Sierra-Alvarez, R. *Environ. Sci. Technol.* **2006**, *40*, 2951–2957.
- Chapman, H. D.; Johnson, Z. B. *Poult. Sci.* **2002**, *81*, 356–364.
- Arai, Y.; Lanzirrotti, A.; Sutton, S.; Davis, J. A.; Sparks, D. L. *Environ. Sci. Technol.* **2003**, *37*, 4083–4090.
- Jackson, B. P.; Seaman, J. C.; Bertsch, P. M. *Chemosphere* **2006**, *65*, 2028–2034.
- Ferguson, A. M.; Hoffmann, M. R.; Hering, J. G. *Environ. Sci. Technol.* **2005**, *39*, 1880–1886.
- Motamedi, S.; Cai, Y.; O'Shea, K. E. Biogeochemistry of Environmentally Important Trace Elements. *ACS Symp. Ser.* **2003**, *835*, 84–94.
- Pettine, M.; Campanella, L.; Millero, F. J. *Geochim. Cosmochim. Acta* **1999**, *63*, 2727–2735.
- Xu, T.; Cai, Y.; Mezyk, S. P.; O'Shea, K. E. Advances in Arsenic Research. *ACS Symp. Ser.* **2005**, *915*, 333–343.
- Xu, T.; Kamat, P. V.; O'Shea, K. E. *J. Phys. Chem. A* **2005**, *109*, 9070–9075.
- Yang, H.; Lin, W. Y.; Rajeshwar, K. *J. Photochem. Photobiol., A* **1999**, *123*, 137–143.
- Dutta, P. K.; Pehkonen, S. O.; Sharma, V. K.; Ray, A. K. *Environ. Sci. Technol.* **2005**, *39*, 1827–1834.
- Lee, H.; Choi, W. *Environ. Sci. Technol.* **2002**, *36*, 3872–3878.
- Ryu, J.; Choi, W. *Environ. Sci. Technol.* **2004**, *38*, 2928–2933.
- Ryu, J.; Choi, W. *Environ. Sci. Technol.* **2006**, *40*, 7034–7039.
- Nakajima, T.; Kawabata, T.; Kawabata, H.; Takahashi, H.; Ohki, A.; Maeda, S. *Appl. Organomet. Chem.* **2005**, *19*, 254–259.
- Maeda, S.; Ohki, A.; Kawabata, T.; Kishita, M. *Appl. Organomet. Chem.* **1999**, *13*, 121–125.
- Atkinson, R.; Darnall, K. R.; Lloyd, A. C.; Winer, A. M.; Pitts, J. N. *Adv. Photochem.* **1979**, *11*, 375–488.
- Cadet, J.; Delatour, T.; Douki, T.; Gasparutto, D.; Pouget, E.; Ravanat, J.; Sauvaigo, S. *Mutat. Res.* **1999**, *424*, 9–21.
- Peller, J.; Wiest, O.; Kamat, P. V. *J. Phys. Chem. A* **2004**, *108*, 10925–10933.
- Pignatello, J. J.; Oliveros, E.; MacKay, A. *Crit. Rev. Environ. Sci. Technol.* **2006**, *36*, 1–84.
- Klaning, U. K.; Bielski, B. H. J.; Sehested, K. *Inorg. Chem.* **1989**, *28*, 2717–2724.
- Buxton, G. V.; Greenstock, C. L.; Helman, W. H.; Ross, A. B. *J. Phys. Chem. Ref. Data* **1988**, *17*, 513–886.
- Ram, M. S.; Stanbury, D. M. *J. Phys. Chem.* **1986**, *90*, 3691–3696.
- Neta, P.; Huie, R. E.; Ross, A. B. *J. Phys. Chem. Ref. Data* **1988**, *17*, 1027–1284.
- Eberson, L. *Adv. Phys. Org. Chem.* **1982**, *18*, 79–185.
- Gordon, S.; Schmidt, K. H.; Hard, E. J. *J. Phys. Chem.* **1977**, *81*, 104–109.
- Asmus, K. D. *Methods Enzymol.* **1984**, *105*, 167–178.
- Schuler, R. H. *Radiat. Phys. Chem.* **1996**, *47*, 9–17.
- Buxton, G. V.; Stuart, C. R. *J. Chem. Soc., Faraday Trans.* **1995**, *91*, 279–281.
- Becke, A. D. *J. Chem. Phys.* **1993**, *98*, 5648–5652.
- Lee, C.; Yang, W.; Parr, R. G. *Phys. Rev. B* **1988**, *37*, 785–789.
- Curtiss, L. A.; Redfern, P. C.; Rassolov, V.; Kedziora, G.; Pople, J. A. *J. Chem. Phys.* **2001**, *114*, 9287–9295.
- Frisch, M. J. T.; Trucks, G. W.; Schlegel, H. B.; Scuseria, G. E.; Robb, M. A.; Cheeseman, J. R.; Zakrzewski, V. G.; Montgomery, J. A., Jr.; Stratmann, R. E.; Burant, J. C.; Dapprich, S.; Millam, J. M.; Daniels, A. D.; Kudin, K. N.; Strain, M. C.; Farkas, O.; Tomasi, J.; Barone, V.; Cossi, M.; Cammi, R.; Mennucci, B.; Pomelli, C.; Adamo, C.; Clifford, S.; Ochterski, J.; Petersson, G. A.; Ayala, P. Y.; Cui, Q.; Morokuma, K.; Malick, D. K.; Rabuck, A. D.; Raghavachari, K.; Foresman, J. B.; Cioslowski, J.; Ortiz, J. V.; Baboul, A. G.; Stefanov, B. B.; Liu, G.; Liashenko, A.; Piskorz, P.; Komaromi, I.; Gomperts, R.; Martin, R. L.; Fox, D. J.; Keith, T.; Al-Laham, M. A.; Peng, C. Y.; Nanayakkara, A.; Gonzalez, C.; Challacombe, M.; Gill, P. M. W.; Johnson, B.; Chen, W.; Wong, M. W.; Andres, J. L.; Head-Gordon, M.; Replogle, E. S.; Pople, J. A. *Gaussian 98*; Gaussian: Pittsburgh, PA, 1998.
- Tchounwou, P. B.; Centeno, J. A.; Patlolla, A. K. *Mol. Cell. Biochem.* **2004**, *255*, 47–55.
- Galvin, R. M. *Aquat. Arsenic Toxic. Treat.* **2003**, 101–112.
- Garelick, H.; Dybowska, A.; Valsami-Jones, E.; Priest, N. D. *J. Soils Sediments* **2005**, *5*, 182–190.
- Jekel, M. R. In *Arsenic in the Environment, Part I: Cycling and Characterization*; Nriagu, J. O., Ed.; John Wiley & Sons, Inc.: New York, 1994; pp 119–132.
- Jiang, J. Q. *Water Sci. Technol.* **2001**, *44*, 89–98.
- Bjergbakke, E.; Sillesen, A.; Pagsberg, P. *J. Phys. Chem.* **1996**, *100*, 5729–5736.
- Mohan, H. *Radiat. Phys. Chem.* **1996**, *49*, 15–19.
- Geeta, S.; Rao, B. S. M.; Mohan, H.; Mittal, J. P. *J. Phys. Org. Chem.* **2004**, *17*, 194–198.
- Chatgililoglu, C.; Ioele, M.; Mulazzani, Q. G. *Radiat. Phys. Chem.* **2005**, *72*, 251–256.
- Armstrong, D. A.; Asmus, K.; Bonifaic, M. *J. Phys. Chem. A* **2004**, *108*, 2238–2246.
- Neta, P.; Hoffman, M. Z.; Simic, M. *J. Phys. Chem.* **1972**, *76*, 847–853.
- Ioele, M.; Chatgililoglu, C.; Mulazzani, M. *J. Phys. Chem. A* **1998**, *102*, 6259–6265.
- Neta, P.; Schuler, R. H. *J. Am. Chem. Soc.* **1975**, *97*, 912–913.
- Singh, T. S.; Gejji, S. P.; Rao, B. S.; Madhava, M.; Hari, M.; Jai, P. *J. Chem. Soc., Perkin Trans. 2* **2001**, *7*, 1205–1211.
- Nicolaescu, A. R.; Wiest, O.; Kamat, P. V. *J. Phys. Chem. A* **2005**, *109*, 2822–2828.
- Alfassi, Z.; Schuler, R. H. *J. Phys. Chem.* **1985**, *89*, 3359–3358.
- Zemel, H.; Fessenden, R. W. *J. Phys. Chem.* **1978**, *82*, 2670–2676.
- Nicolaescu, A. R.; Wiest, O.; Kamat, P. V. *J. Phys. Chem. A* **2003**, *107*, 54.
- Mohan, H.; Mittal, J. P. *J. Phys. Chem. A* **1999**, *103*, 379–383.
- Merga, G.; Aravindakumar, C. T.; Rao, B. S. M.; Mohan, H.; Mittal, J. P. *J. Chem. Soc., Faraday Trans.* **1994**, *90*, 597–604.